Acta Geologica Sinica (English Edition), 2019, 93(6): 1797–1807

He–Ar Isotopic Tracing of Pyrite from Ore-forming Fluids of the Sanshandao Au Deposit, Jiaodong Area

HAN Zhenyu[1, 2], YU Xiaowei[3], LI Shoujun[1, *], Tian Jingxiang[4, 5, 6], WANG Zhongliang[7], YU Xiaojing[8] and WANG Ligong[3]

[1] *College of Earth Science & Engineering, Shandong University of Science and Technology, Qingdao, Shandong 266590, China*
[2] *Yantai Natural Museum, Yantai, Shandong 264000, China*
[3] *Shandong Institute of Geological Survey, Ji'nan 250014, China*
[4] *Shandong Institute of Geological Sciences, Ji'nan 250014, China*
[5] *Key Laboratory of Gold Mineralization Process and Resources Utilization, Ministry of Land and Resources Ji'nan 250014, China*
[6] *Key Laboratory of Metal Mineralization Geological Processes and Resources Utilization in Shandong Province Ji'nan 250014, China*
[7] *State Key Laboratory of Geological Process and Mineral Resources, China University of Geosciences, Beijing 100083 China*
[8] *The third Exploration Institute of Geology and Mineral Resources of Shandong Province, Yantai, Shandong 264000, China*

Abstract: The Sanshandao Au deposit is located in the famous Sanshandao metallogenic belt, Jiaodong area. To date, accumulative Au resources of 1000 t have been identified from the belt. Sanshandao is a world-class gold deposit with Au mineralization hosted in Early Cretaceous Guojialing-type granites. Thus, studies on the genesis and ore-forming element sources of the Sanshandao Au deposit are crucial. He and Ar isotopic analyses of fluid inclusions from pyrite (the carrier of Au) indicate that the fluid inclusions have $^{3}He/^{4}He$=0.043–0.21 Ra with an average of 0.096 Ra and $^{40}Ar/^{36}Ar$=488–664 with an average of 570.8. These values represent the initial He and Ar isotopic compositions of ore-forming fluids for trapped fluid inclusions. The comparison of H–O isotopic characteristics combined with deposit geology and wall rock alteration reveals that the ore-forming fluids of the Sanshandao Au deposit show mixed crust–mantle origin characteristics, and they mainly comprise crust-derived fluid mixed with minor mantle-derived fluid and meteoric water during the uprising process. The ore-forming elements were generally sourced from pre-Cambrian meta-basement rocks formed by Mesozoic reactivation and mixed with minor shallow crustal and mantle components.

Key words: Sanshandao Au deposit, He and Ar isotopes, fluid inclusions, crustal fluid, mantle-derived fluid

Citation: Han et al., 2019. He–Ar Isotopic Tracing of Pyrite from Ore-forming Fluids of the Sanshandao Au Deposit, Jiaodong Area. Acta Geologica Sinica (English Edition), 93(6): 1797–1807. DOI: 10.1111/1755-6724.14335

1 Introduction

The Sanshandao Au deposit is located in the famous Sanshandao Au metallogenic belt, Jiaodong area, and it is a typical Jiaodong-style Au deposit (Zhai Mingguo et al., 2001; Yang Liqiang et al., 2014; Song Mingchun et al., 2015a). Sanshandao is a world-class Au deposit with Au mineralization hosted in Early Cretaceous Guojialing-type granites, as well as one of the largest Au deposits in the giant Jiaodong Au metallogenic province (Deng et al., 2010). In recent years, with the discovery of ultra large gold deposits in the northern waters of Sanshandao and the Xiling Au deposit, which are controlled by the Sanshandao fault belt, the accumulative Au resources that have been identified in the Sanshandao Au metallogenic belt have exceeded 1000 t. The belt plays an important role in the three large metallogenic belts of Jiaodong. Therefore, research on the genesis and ore-forming element sources of the Sanshandao Au deposit is crucial. However, explanations about the sources of ore-forming fluids of Au deposits in the Jiaodong area vary; the possible sources mainly include post-magmatic hydrothermal mineralization (An et al., 1988; Yao et al., 1990; Li et al., 1993; Li et al., 2006), metamorphic hydrothermal mineralization (Shen, 1994; Li et al., 1995), hydrothermal reactivation mineralization of deep meteoric water circulation (Zhang, 1989; Yang et al., 1991), and mixed crust–mantle-derived fluid mineralization (Deng et al., 2000; Yang et al., 2000; Zhang et al., 2002; Mao et al., 2005).

Rare gases, particularly He and Ar, have stable isotopic chemical properties but extremely variable isotopic compositions in crust and mantle reservoirs. Research into the rare gases of deposits is a hotspot in modern geosciences, and the isotopic composition of rare gases is of great significance to uncover the sources, genesis, and

* Corresponding author. E-mail: lishoujun@126.com

© 2019 Geological Society of China

evolution of ore-forming fluids. The degree of gas leakage of pyrite is much lower than that of other minerals. Isotopic fractionation induced by dispersion and loss of He and Ar from fluid inclusions and epigenetic superimposition of He and Ar can be neglected (Hu et al., 1999). Through He and Ar isotopic analyses of fluid inclusions in pyrite and comparison of H and O isotopes of quartz grains, the sources and evolution of ore-forming fluids of the Shanshandao Au deposit were analyzed.

2 Geological Setting

2.1 Regional geology

The Sanshandao Au deposit is located in the northwest of Jiaodong Peninsula, near Sanshan Island, approximately 20 km NNE of Laizhou City, and geotectonically within the Jiaobei faulted uplift (IV), Jiaobei uplift (III), Jiaoliao uplift region (II), and North China Plate (I). Northwestern Jiaodong lithologically consists of pre-Cambrian metamorphic rocks and Mesozoic–Cenozoic geological bodies (Fig. 1). The pre-Cambrian metamorphic rocks comprise the Neoarchean granite–greenstone belt, which is composed of dominant TTG gneiss and secondary meta-gabbros, with minor residual enclaves of the Neoarchean Jiaodong Group, Mesoarchean Tangjiazhuang Group, and Paleoproterozoic Jingshan and Fenzi Groups. The Mesozoic geological bodies principally include Jurassic Linglong-type granites (163–155 Ma; zircon U–Pb age; Yang et al., 2012; Ma et al., 2013), Cretaceous Guojialing-type gzranites (132–123 Ma; zircon U–Pb age; Wang et al., 2014; Liu et al., 2014), Weideshan-type granites (120–113 Ma; zircon U–Pb age; Goss et al., 2010; Li et al., 2012), Laoshan-type granites (115.4–90 Ma), and acidic and medium-basic dykes. Among the fault systems that control gold deposits in northwestern Jiaodong, the NNE–NE trending ore-controlling fault system is the most important one and directly controls ultra large and large Au deposits and most medium–small Au deposits within the area. The three main ore-controlling faults from west to east are the Sanshandao, Jiaojia, and Zhaoping faults. Northwestern Jiaodong is under a tectonic framework constituted by multi-phased, polygenetic magmatic activities and predominant NE-trending fault structures.

2.2 Deposit geology

Accumulative Au reserves of 200 t have been identified from the Sanshandao Au deposit. Currently, 52 t of Au reserves have been mined, and the annual production is approximately 8 t (data sourced from Shandong Gold Group Co., Ltd.). The deposit is controlled by the Sanshandao fault, which is located in the west end of the Jiaodong Au cluster area. The fault is merely outcropped at the surface locally and mostly covered by Quaternary sediments. The fault extends from Sanshandao Town southwestwards to Panjiawuzi, with two ends extending into the Bohai Sea. The southwestern end of the fault is outcropped again at Furong Island after extending into sea. The fault has an outcropped length of 12 km and a width of 50–200 m in the land, and it occurs as an "S" shape in plain view. The fault generally strikes 40° with local 70–80° and dips to SE at 45–75°. The fault chiefly spreads along contact between the Guojialing-type monzonitic granites (data not published) and the Qixia, Huilongkuang Unit banded biotite tonalitic gneiss (including meta-gabbro enclaves). It is lithologically composed of mylonite, cataclasite, and cataclastic rocks; has a continuous, stable major fracture surface; and shows compressoshear signature.

Previous scholars used mineralization characteristics to divide gold deposits in northwestern Shandong Peninsular into fractured-zone altered rock type (Jiaojia type), quartz

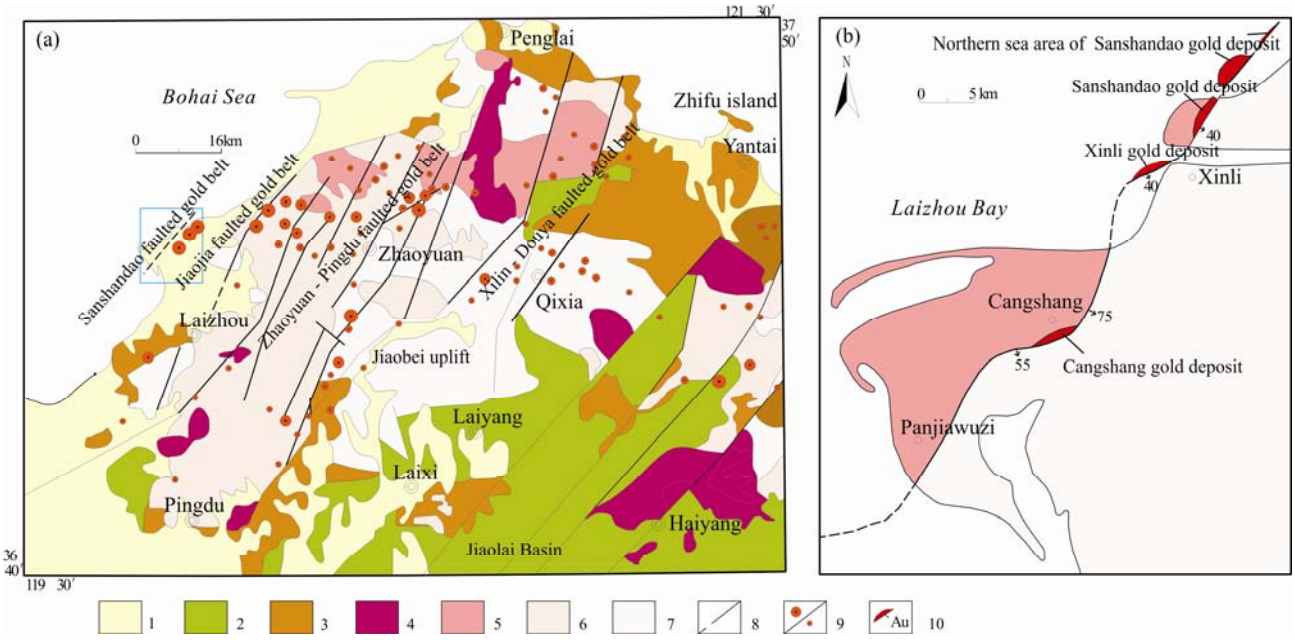


Fig. 1. Geological map of northwestern Shandong Peninsula (a) and bedrocks of nearby regions of the Sanshandao fault (b).
1-Quanternary; 2-Cretaceous; 3-Palaeoproterozoic; 4-Cretaceous Weideshan-type granites; 5-Cretaceous Guojialing-type granites; 6-Jurassic Linglong-type granites; 7-Archean TTG (including meta-gabbro enclaves); 8-Measured and inferred fault; 9-Ultralarge, large/medium–small Au deposit; 10-Au ore body.

vein type (Linglong type), and transitional type (altered rock type+quartz vein type) (Zhang et al., 1988; Lv and Yang, etc. 1993; Yang et al., 1996; Hu et al., 1998). Mineralization types within the Sanshandao fault belt are divided into fractured-zone altered rock and vein types depending on ore body shape, attitude, and occurrence location. On the basis of ore-controlling factors, ore texture–structure and type, and wall rock alteration, the fractured-zone altered rock type can be further divided into phyllic rock, silicified rock, and potash alteration rock subtypes. Moreover, vein type can be further categorized into silicified vein, vein-like phyllic, and quartz–sulfide vein subtypes (Fig. 2).

No. ①-1 is the dominant ore body and occurs as an asymmetric Z-shaped irregular vein, showing divergence, convergence, swelling, shrinkage, wedge-out, and reoccurrence. In general, the ore body strikes approximately 35° and dips to SE at 34–44°. The ore body thickness is 0.95 at minimum, 12.08 at maximum, and 6.65 m at average. The thickness variation coefficient is 68.9%, which indicates a stable thickness type (the aforementioned values are calculated by the accumulative single-engineering thickness of multiple layers). The ore body extends discontinuously along striking or dipping and shows wedge-out and reoccurrence characteristics. The single-sample Au grade of the ore body is 15.40 ppm (ZK48-2) at maximum. The single-engineering Au grade varies from 1.74 ppm to 5.65 ppm with an average of 3.25 ppm and a grade variation coefficient of 70.6%, indicating homogeneous grade distribution (Fig. 3).

In this paper, hydrothermal mineralization of the Au deposit is divided into pyrite–quartz–sericite, gold–quartz–pyrite, gold–quartz–polymetallic sulide and quartz–calcite stages.

1) pyrite-quartz-sericite stage: is the early stage of gold mineralization and marked by sericite or quartz–pyrite veins; 2) gold–quartz–pyrite stage: is the major mineralization stage of the area and characterized by quartz–pyrite veinlets and stockworks within the phyllic alteration zone or by Au-bearing quartz–pyrite veins filled within secondary faults; 3) gold–quartz–polymetallic sulfide stage: is a significant mineralization stage and mainly characterized by veinlet-disseminated mineralization, filled with veinlets that cut through the quartz–pyrite veins of Stage II, or by veinlet-stockworked mineralization within dessiminated ores; 4) quartz-calcite stage： In this stage, quartz calcite vein is formed, which is superimposed on the earlier mineralized products, and cuts through quartz pyrite veinlets or quartz polymetallic sulfide vein in disseminated ore. No gold minerals were found at this stage.

2.3 Characteristics of fluid inclusions

In the Sanshandao Au deposit, fluid inclusions are mainly hosted in quartz. Quartz samples were collected from ore veins of variable mineralization stages or ore types of the same mineralization stage. Quartz contains many types of fluid inclusions. Most of the fluid inclusions are colorless and transparent, and low amounts of inclusions bearing organic gases such as carbon are brownish black. The fluid inclusions are generally regular or irregular. Regular inclusions are dominated by rounded, elliptical, and negative crystals. Irregular inclusions are dominated by elongated banded, crescent, and spoon shapes. They are small and mostly <10 μm in diameter, clustering from 2 μm to 7 μm. Several large inclusions



Fig. 2. Ore characteristics of the Sanshandao Au deposit.
(a) Silicified vein ore type; (b) Vein-like quartz–sulfide ore type; (c) Beresitized cataclasite ore type; (d) Beresitized granitic cataclasite ore type.

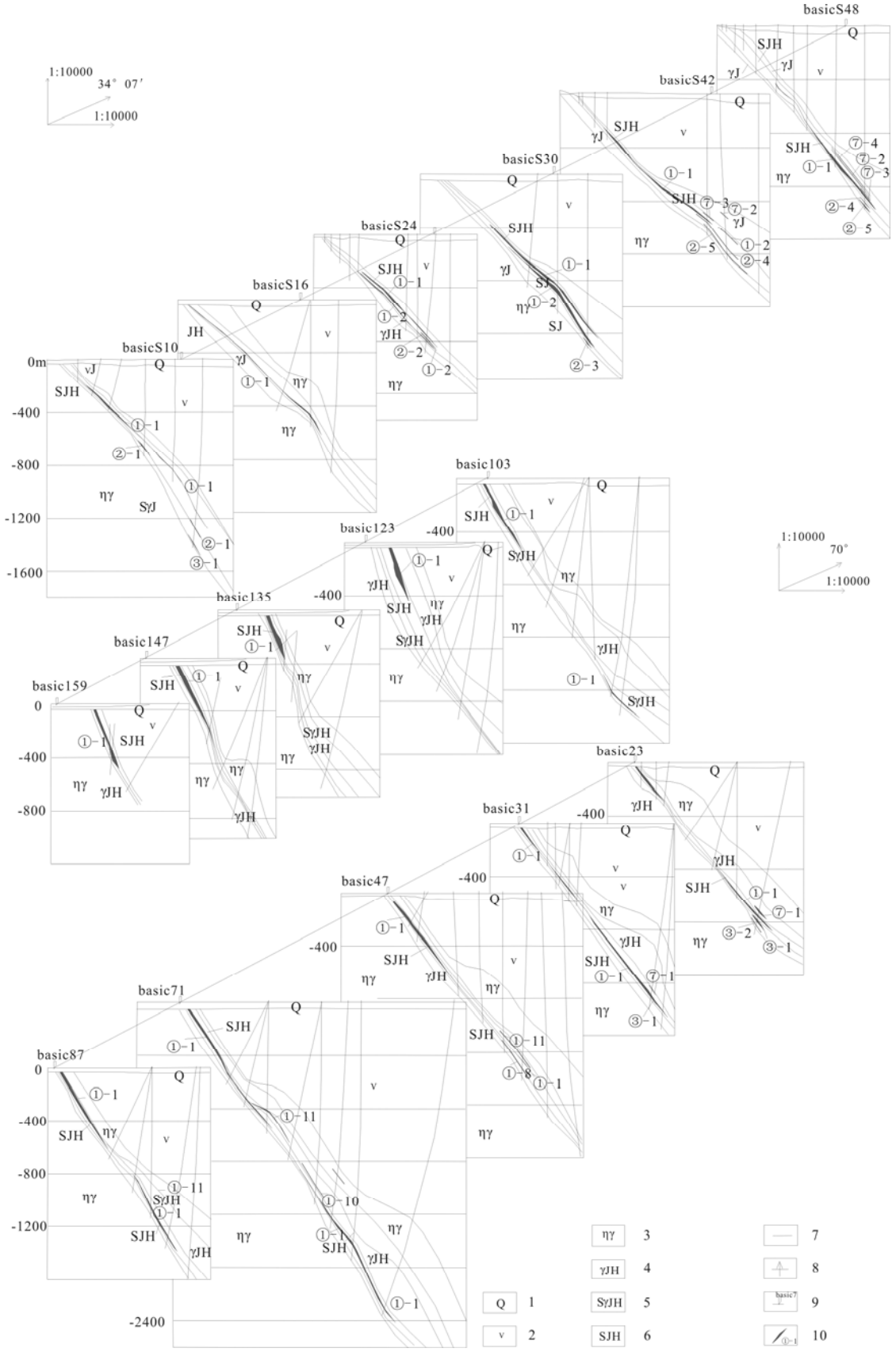


Fig. 3. Combined section of Orebody ①-1.

1-Quaternary; 2-Metagabbro; 3-Monzonitic granite; 4-Beresitized granite; 5-Beresitized granitic cataclasite; 6-Beresitized cataclasite; 7-Drift; 8-Drillhole; 9-Base point with ID; 10-Ore body with ID.

have diameters of up to 15 μm. Fluid inclusions in host minerals of variable types and origins show obvious size distribution laws. Fluid inclusions of the Sanshandao Au deposit consist of vapor and liquid phases. Considering phase composition, percentage, and the relationship of various phases of fluid inclusions at room temperature, fluid inclusions of the deposit area can be divided into three types: single-phase (I type), two-phase (II type), and three-phase inclusions (III type). Characteristics of the various types of fluid inclusions are shown in Fig. 4 and Table 1 (Hu et al., 2000; Wang et al., 2015).

3 Sampling and Analytical Methods

Five samples were collected from underground works and drillholes of the Sanshandao Au deposit for this study, including three from −135 m and −390 m levels and two from ore-intersected drillholes. Fluid inclusions of pyrite from various ore types of early, major, and late mineralization stages were tested. Individual pyrite minerals were separated from Au-bearing ores using the panning method, and >500 mg of 40–60 mesh sample was selected to have >99% of pyrite using a binocular microscope (sample selection was accomplished in Langfang Geosciences Exploration Technical Service Co., Ltd.). Pyrite He and Ar isotopic analyses were completed at the Lanzhou Research Center of Oil and Gas Resources, Institute of Geology and Geophysics, Chinese Academy of Sciences on a Noblesse mass spectrometer (produced by Britain Nu). Instrument parameters were as follows: high pressure of 7.0 kV and trap electric current of 400 (for Ne, Ar, and Xe) and 500 mA (for He). ^{4}He, Ne, and Ar were tested using Faraday Cup, whereas ^{3}He, Kr, and Xe were tested using an ion counter. Clean air collected from the suburbs was used as the standard sample. Air has ^{4}He=1.10E-14, an Ar content of 0.934%, ^{4}He/^{20}Ne= 0.3185, Ra=^{3}He/^{4}He=1.400E-06, ^{38}Ar/^{36}Ar= 0.1880, and ^{40}Ar/^{36}Ar=295.5. The LDB03-01-2016 rare-gas isotopic mass spectrometry peak/height ratio method was employed as testing basis. More details can be found in the literature (Chunhui Cao et al., 2018).

4 Analytical Results

He and Ar isotopic analytical results of fluid inclusions from pyrite of the Sanshandao Au deposit are shown in Table 2.

5 Discussion

5.1 He and Ar isotopic characteristics

The pyrites in the samples are mostly semi-automorphic, automorphic and irregular grains. They are disseminated in sericite or filled in fissures in vein shape. The main particle size ranges from 0.01 mm to 2 mm. Generally, the parts rich in fine pyrite have higher gold grade. It can be divided into early and late generations. Early generation pyrite is irregular granular, a small amount of cubic automorphic crystals is distributed in quartz, sericite and other minerals. Owing to hydrothermal modification and stress in later period, it is often crushed, cracks develop, and metasomatized by late fine pyrite and arsenopyrite, or filled with late generation pyrite, presenting crushing structure. Coarse-grained pyrite often contains chalcopyrite, pyrrhotite and other minerals, or is intersected by galena and chalcopyrite veins in the gold-bearing polymetallic sulfide stage. Late-generation fine-grained pyrite is also veined and reticulated with chalcopyrite, galena and arsenopyrite in quartz and early pyrite.

The fluid inclusions of pyrite analyzed by the institute are dominated by primary inclusions; thus, the influence from late-stage diffusion and loss can be excluded. Pyrite samples analyzed by the institute were all collected from underground works and drillholes, so the possibility that cosmogenic ^{3}He exists in fluid inclusions can be ignored. Given that Li-bearing minerals are absent in the area, the influence from the epigenetic superimposition of radiogenic ^{3}He can be excluded. The analyses show that fluid inclusions of pyrite in the samples have F^{4}He=7082–28392, which is much higher than 1 (Kendrick et al., 2001; Mao et al., 2005); therefore, atmosphere contamination on He in fluid inclusions can be disregarded. Inert gases in hydrothermal solution may have four sources: 1) atmospheric saturated water, including meteoric water and sea water, and its typical He and Ar isotopic composition is ^{3}He/^{4}He=1Ra (Ra represents atmospheric He ^{3}He/^{4}He=1.4 ppm), ^{40}Ar/^{36}Ar=295.5; 2) mantle-derived fluid, with high ^{3}He concentration, ^{3}He/^{4}He clustering from 6 Ra to 9 Ra, and greatly variable ^{40}Ar/^{36}Ar, generally >40,000; 3) crustal radiogenic He and Ar; the ratio of ^{3}He/^{4}He typically varies from 0.01 Ra to 0.05 Ra, and the ratio of ^{40}Ar/^{36}Ar is also high; and 4) atmospheric He and Ar; as the content of He is very low in the atmosphere and insufficient to affect the

Table 1 Composition and development characteristics of different fluid inclusions

Type	Sub-type	Vapor/liquid ratio	Composition	Main development stage
Single phaseinclusion (I type)	Pure liquid-phase inclusion (I-l type)	—	Saline solution	Moderate-late mineralization stage
	Pure vapor-phase inclusion (I-g type)	—	Vapor CO_2+CH_4	Early mineralization stage
Two-phase inclusion (II type)	Two-phase inclusion (II-l type)	L/(V+L)>50%	Saline solution, vapor H_2O, vapor CO_2+CH_4	Moderate-late mineralization stage
	Two-phase inclusion (II-g type)	V/(V+L)>50%	Saline solution, vapor H_2O, vapor CO_2+CH_4	Moderate-late mineralization stage
	Double liquid-phase inclusion (II-2l type)	$L_{CO2}/L_{H2O+CO2}$ 5%–20%	Saline solution, liquid CO_2	Early-moderate mineralization stage
Three-phase inclusion (III type)	CO_2 three-phase inclusion (III CO_2 type)	$V_{CO2}+L_{CO2}$/ V+L 35%–55%	Saline solution, liquid CO_2, vapor CO_2+CH_4	Early-moderate mineralization stage

Table 2 He and Ar isotopic compositions of fluid inclusions of pyrite from gold deposits in the Jiaodong area

Deposit	Sample ID	$^{40}Ar/^{36}Ar$	$^{3}He/^{4}He$ (10^{-6})	$^{40}Ar\times10^{-7}$ (cm^3STP/g)	$^{4}He\times10^{-7}$ (cm^3STP/g)	R/Ra	$^{40}Ar^*$ (%)	F^4He	$^{40}Ar^*/^4He$	Mantle-derived He (%)	Data source
Sanshandao	135M-TW1	664	0.068	17.37	138	0.0484	55.50	31876.37	0.13	0.4344	This study
	390-TW1	488	0.169	8.91	33.9	0.1207	39.45	11220.86	0.26	1.3570	
	390-TW2	529	0.296	9.48	21.0	0.2114	44.14	7081.45	0.45	2.5137	
	HZK8401TW3	562	0.076	15.37	101	0.0543	47.42	22317.79	0.15	0.5100	
	HZK8401TW4	611	0.061	18.46	142	0.0434	51.64	28392.36	0.13	0.3707	
Cangshan	Csh1	425±2	2.29±0.41	5.7	2.11	1.64	30.47	950.60	0.82	20.67	Mao et al., 2005
	Csh2	382±1	1.56±0.09	14.21	5.27	1.11	22.64	856.02	0.61	14.03	
	Csh5	284±2	1.91±0.28	23.14	1.31	1.36	0.00	97.15	—	17.21	
	Csh6	445±1	1.82±0.14	8.66	8.06	1.3	33.60	2502.53	0.36	16.39	
	Csh7	357±2	1.45±0.13	16.69	4.88	1.04	17.23	630.72	0.58	13.02	
Jiaojia	JJ-190-2	719±19	2.51±0.38	2.94	2.33	1.79	58.90	3443.02	0.74	22.68	Mao et al., 2005
	JJ-190-10	512±1	3.02±0.47	25.34	9.32	2.16	42.29	1137.84	1.15	27.32	
	JJ-190-13	363±4	1.33±0.28	13.61	7.27	0.95	18.60	1171.62	0.35	11.93	
	JJ-190-14	516±2	2.86±0.52	5.50	3.22	2.04	42.73	1825.35	0.73	25.87	
	Jjia3	350±2	1.06±0.21	6.59	4.12	0.76	15.57	1322.15	0.25	9.47	
Zhaodaoshan	Zk16-2-2	429	0.056	8.10	36.90	0.0433	31.12	11808.66	0.22	0.33	Zhang, 2010
	Zk16-3-1	393	0.504	4.16	5.70	0.36	24.81	3253.69	0.73	4.41	
	Zk16-3-5	6946	0.378	2.30	3.23	0.27	95.75	58940.18	0.71	3.26	
	Zk80-2-1	794	0.098	2.42	9.29	0.08	62.78	18417.17	0.26	0.71	
	Zk120-1-1	1637	0.140	3.10	20.30	0.10	81.95	64771.66	0.15	1.09	
Jinqing ding	JQD-KD-2	475	0.651	3.36	3.43	0.47	37.79	2929.88	0.98	5.75	Chen, 2010
	JQD-785-3	463	3.073	1.05	0.42	2.2	36.18	1119.03	2.50	27.81	
	JQD-585-13	728	0.133	2.39	6.41	0.1	59.41	11797.60	0.37	1.03	
	JQD-635-01	981	0.160	1.08	4.01	0.12	69.88	22008.56	0.27	1.28	
	JQD-B10	1508	0.177	2.2	9.65	0.13	80.40	39967.59	0.23	1.43	
Yingge zhuang	YGZS115-2	1877	0.052	4.15	101.1	0.04	84.26	276292.65	0.04	0.30	Zhou, 2010
	YGZS115-14	463	0.280	7.38	29.7	0.2	36.18	11258.57	0.25	2.37	
	YGZN80-16	690	0.496	12.90	25.6	0.36	57.17	8273.73	0.50	4.34	
	YGZS75-2	636	0.525	5.55	12.92	0.38	53.54	8945.99	0.43	4.60	
	YGZN80-30	643	0.571	4.73	4.16	0.41	54.04	3417.00	1.14	5.02	

He isotopic composition of crustal fluid. However, it is impossible to identify whether the fluid is mixed with atmospheric Ar (Stuart et al., 1995).

Among the five samples, fluid inclusions from pyrite have $^{3}He/^{4}He$=0.043–0.21 Ra, with an average of 0.096 Ra, slightly higher than the value (0.01–0.05 Ra) of crustal material (Stuart F M, 1995; Burnard P G, 1999) but obviously lower than that (6–9 Ra) of typical mantle material (Stuart F M, 1995; Burnard P G, 1999). A ^{3}He–^{4}He isotopic evolution diagram (Fig. 5) shows that He isotopic compositions of the ore-forming fluid plot are within the transitional field from crust to mantle compositions and close to crustal composition. The $^{3}He/^{4}He$ ratio varies from 10^{-6} to 10^{-7}, showing signatures of mixed mantle–crust composition. If the ore-forming fluid is a simple binary mixed crust–mantle model, then the ^{3}He /^{4}He ratios can be used to derive the ratio of mantle-derived fluid (R_m)/crustal fluid (R_c) in the fluid. The percentage of mantle-derived He can be calculated using the following formula: mantle-derived He(%)=[(R-R_c)/(R_m–R_c)]×100, R_c end-member value=2×10^{-8}, and R_m end-member value=1.1×10^{-5} (Li et al., 2003). The calculation indicates that fluid inclusions in pyrite of the Sanshandao Au deposit have mantle-derived He between 0.37% and 2.51% with an average of 1.04%, implying that He of the Au ore-forming fluids was mainly sourced from crustal He, with low amounts of mantle-derived He. Fluid inclusions in pyrite from the Zhaodaoshan Au deposit (quartz vein type) have $^{3}He/^{4}He$=0.04–0.36 R/Ra, with an average of 0.17 R/Ra, between crustal He and mantle-derived He. The percentage of mantle-derived fluid involved in mineralization varies from 0.33% to 4.41%, and that of crust-derived fluid is predominant (Zhang, 2010). Fluid inclusions in pyrite from the Jinqingding Au deposit (quartz vein type) have $^{3}He/^{4}He$=0.1–2.2 R/Ra, with an average of 0.60 R/Ra, between crust-derived He and mantle-derived He. Mantle-derived He in the fluid inclusions of pyrite accounts for 1.03%–27.81%, which is consistent with the results of the study (Mao et al., 2008).

The fluid inclusions in pyrite have $^{40}Ar/^{36}Ar$=488–664, with an average of 570.8, and ^{40}Ar varies within (8.93–18.5)$\times10^{-7}$ cm^3STP/g. The $^{40}Ar/^{36}Ar$ ratio is approximately twice of the $^{40}Ar/^{36}Ar$ ratio (298). This result indicates that crustal radiogenic Ar ($^{40}Ar^*$) exists in the fluid. The percentage of radiogenic Ar was calculated to vary from 39.45% to 55.50%, with an average of 47.63%. The He and Ar isotopic composition plot on a R/Ra–$^{40}Ar/^{36}Ar$ diagram (Fig. 6), near the crust-derived fluid field, with injected atmosphere precipitation and mantle-derived fluids, suggests that the ore-forming fluid is dominated by

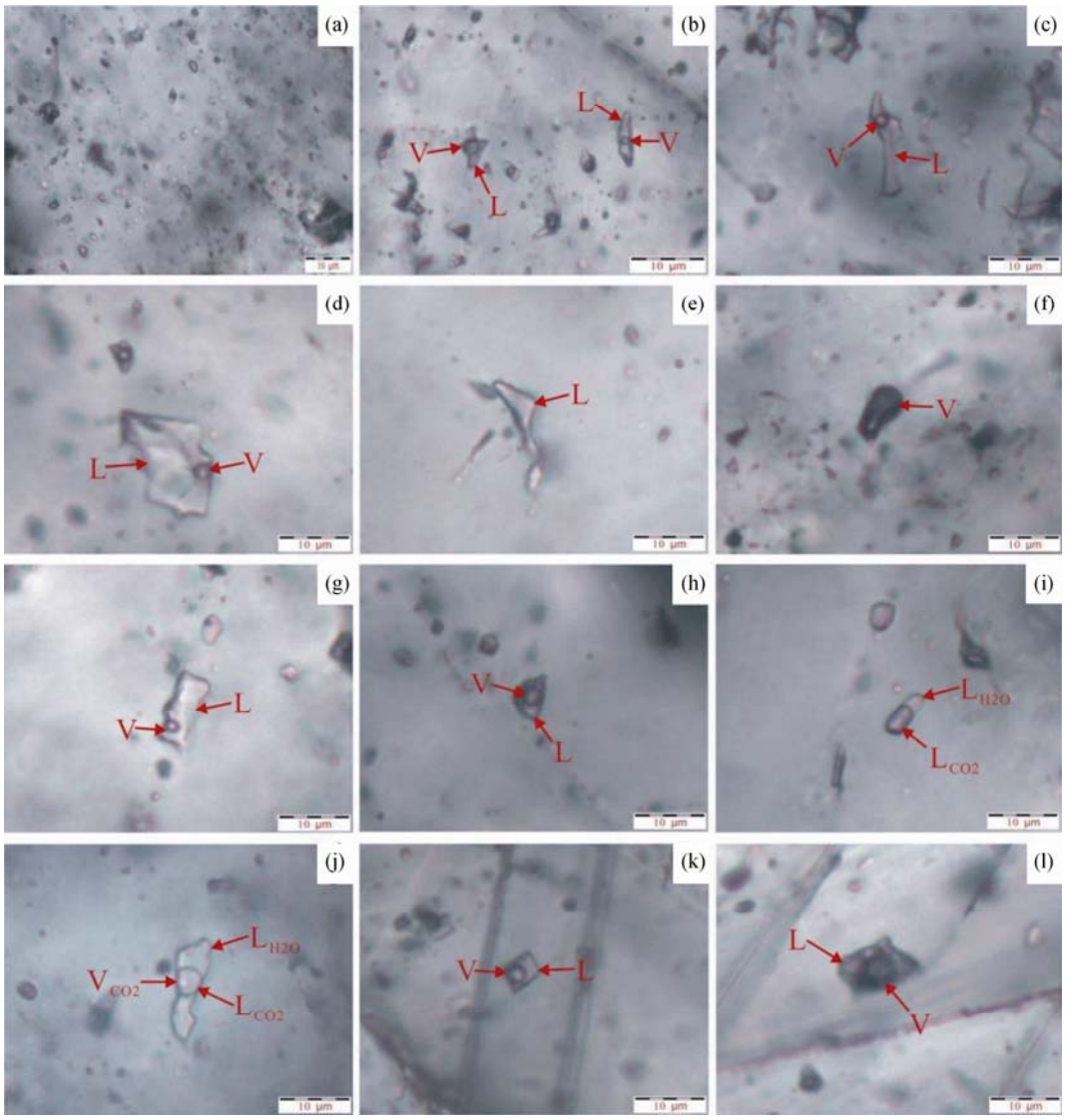


Fig. 4. Characteristics of fluid inclusions from the Sanshandao Au Deposit.
(a) round and round-like inclusion group in quartz; (b) irregular inclusion group in quartz; (c) elongated inclusions in quartz; (d) irregular two-phase inclusions in quartz; (e) I-1-type inclusions in quartz; (f) I-g-type inclusions in quartz; g-II-l-type inclusions in quartz; (h) II-g -type inclusions in quartz; (i) II-2l-type inclusions in quartz; (j) IIICO_2- type inclusions in quartz; (k) II-l-type inclusions in quartz; (l) II-g- type inclusions in calcite.

crust-derived fluid mixed with meteoric water and mantle-derived fluid. The ratio of $^{40}Ar^*/^4He$ varies from 0.13 to 0.45, with an average of 0.22, which is slightly higher than the crustal value (0.156) and lower than the mantle value (0.33–0.56) (Stuart et al., 1995; Hu et al., 1997a). Existing research has indicated that underground water capturing radiogenic ^{40}Ar and ^4He from the crust is correlated with the closure temperatures of He and Ar. For most minerals, the closure temperature of He is very low (200°C), whereas that of Ar is much higher (>200°C) (Ballentine et al., 2002). In the area, the end-member $^{40}Ar^*/^4He$ ratio of crust-derived fluid in the ore-forming fluids is higher than that of normal crust-derived fluid. Meteoric water trapped some radiogenic ^{40}Ar during the major mineralization stage, and the temperature of the ore-forming fluids was high (>200°C); this is consistent with the actual major mineralization stage temperature (170–335°C, generally >200°C) of the area (Fan et al., 2005). Therefore, the ore-forming fluid of the area was principally sourced from the crust and contaminated with deep mantle-derived fluid at a variable degree. Meteoric water participated in the uplifting process of the ore-forming fluid (B.R.HACKER, 2009).

5.2 H and O isotope characteristics

The complete homogenization temperatures of CO_2-H_2O of Ⅱ-l, Ⅱ-g and ⅢCO_2 -type inclusions from the Sanshandao Au Deposit were tested; the results indicate that the complete homogenization temperatures of fluid inclusions from the area varied from 139.7°C to 437.8°C, with a concentration of 180°C–340°C and minor of <180°C and >340°C. Generally, the temperature data indicate moderate-low temperature ore-forming fluids (Wang et al., 2016).

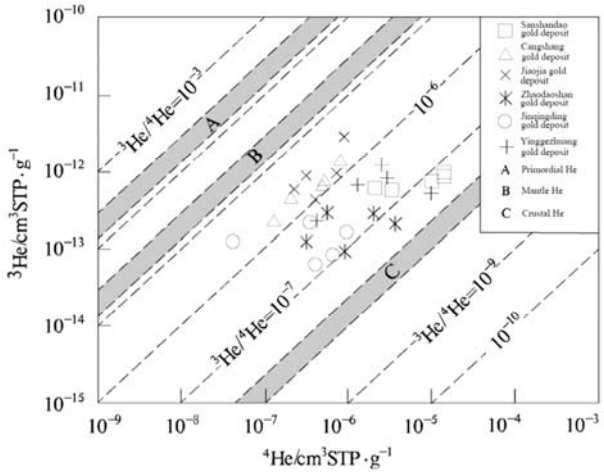


Fig. 5. He isotope composition of fluid inclusions in pyrite from the Sanshandao gold deposit and the deposits in the Jiaodong area (the base map was modified after Mamyrin et al., 1984).

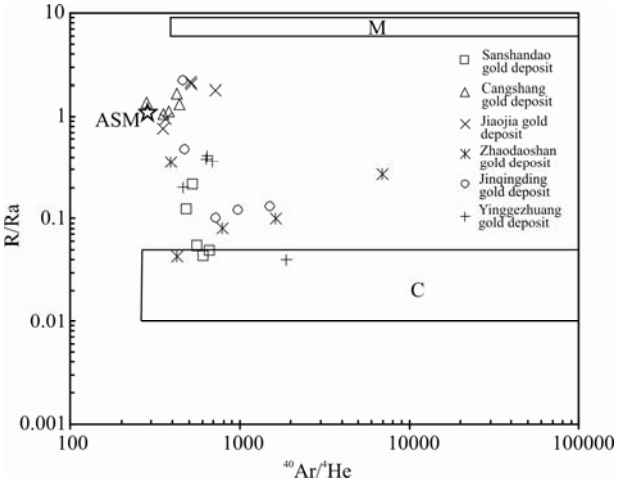


Fig. 6. $^{40}Ar/^{36}Ar$-R/Ra diagram of fluid inclusions in pyrite from gold deposits in Sanshandao and the other Jiaodong area (the base map was modified after Duan et al., 2016). ASM.-Atmospheric saturated water; M.-Mantle-derived fluid range; C.-Crustal fluid range.

Quartz H–O isotopes of the Sanshandao Au deposit have $\delta^{18}O_{Q\text{-}SMOW}$=13.1‰–15.1‰ with an average of 14.4‰, and calcite He and O isotopes have $\delta^{18}O_{C\text{-}SMOW}$ =11.4‰–12.2‰, with an average of 11.9‰. On the basis of the homogenization temperatures of fluid inclusions from the tested samples, calculation using the mineral water O isotopic fractionation equation shows that the ore-forming fluid has $\delta^{18}O_{W\text{-}SMOW}$=1.0‰–8.5‰, with an average of 5.26‰. In this analysis, water of fluid inclusions from the Sanshandao Au deposit has δD=−69.2‰ to −82.1‰, with an average of −75.1‰.

H and O isotopic testing includes samples of four mineralization stages of the Sanshandao Au deposit; fluid inclusions of Mineralization Stage I have $\delta^{18}O_{W\text{-}SMOW}$=8.3‰–8.5‰ with an average of 8.4‰ and δD=−69.2‰ to −71.5‰, with an average of −70.3‰; fluid inclusions of Mineralization Stage II have $\delta^{18}O_{W\text{-}SMOW}$=5.3‰–6.9‰ with an average of 6.3‰ and δD=−71.1‰ to −73.8‰, with an average of −72.3‰; fluid inclusions of Mineralization Stage III have $\delta^{18}O_{W\text{-}SMOW}$=5.0‰–5.8‰ with an average of 5.4‰ and δD=−71.2‰ to −79.5‰ with an average of −75.4‰; fluid inclusions of Mineralization Stage IV have $\delta^{18}O_{W\text{-}SMOW}$=1.0‰–4.9‰ with an average of 2.9‰ and δD=−74.4‰ to −82.1‰ with an average of −79.6‰. Accordingly, from the early to late mineralization stages, fluid inclusions have $\delta^{18}O_{W\text{-}SMOW}$, and δD gradually decreases (Deng et al., 2015) (Table 3).

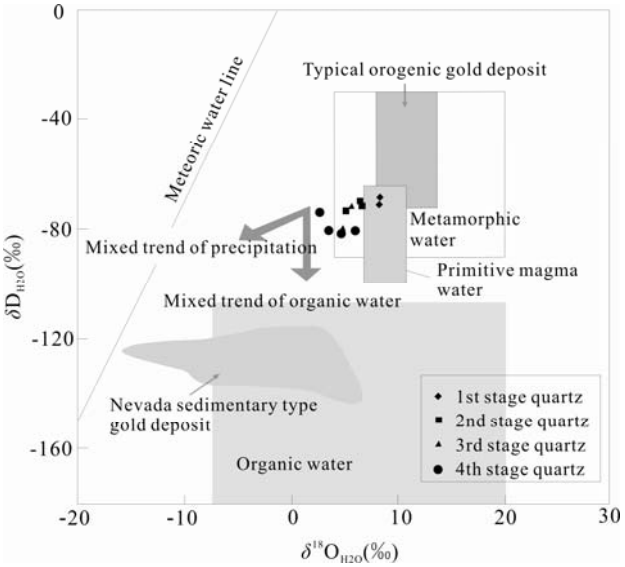


Fig. 7. δD-δ^{18}O diagram of ore-forming fluids from gold deposits in Sanshandao and Jiaodong area(the base map was modified after Taylor,1974; Sheppard, 1977).

H and O isotopic values are plotted on the ore-forming fluid δD–δ^{18}O correlation diagram (Fig. 7) proposed by Taylor (1974). This diagram shows that the H and O isotopic compositions of mineralization stages I and II mainly fell within the magmatic water field, whereas those of mineralization stages III and IV mainly fell within the left part of the magmatic water field. From the early to late mineralization stages, H and O isotopic values decreased slightly and gradually fell near the meteoric water line. Therefore, ore-forming fluids of the early mineralization stage were mainly magmatic water. With the evolution of ore-forming fluids, meteoric water was injected gradually in the late stage, and the fluids were continuously separated. Thus, temperature decreased continuously, and massive amounts of Au precipitated from the fluids.

Accordingly, early-stage ore-forming fluids of the Sanshandao Au deposit were chiefly magmatic hydrothermal solution. The major mineralization stage was dominated by magmatic hydrothermal solution mixed with meteoric water. In the late mineralization stage, the amount of meteoric water mixed with ore-forming fluids gradually increased.

5.3 S and Pb isotopes

The pyrite $\delta^{34}S$ values are 10.9‰ and 10.9‰–11.5‰ respectively in Mineralization Stages I and II of the

Table 3 Hydrogen and oxygen isotopic compositions of the ore-forming fluid from the Sanshandao Au deposit

Sample ID	Mineral	Mineralization stage	$\delta^{18}O_{mineral}$ (‰) $_{SMOW}$	$\delta^{18}O_{water}$(‰)$_{SMOW}$	Homogenization temperature(°C)	δD(‰)$_{SMOW}$	Data source
S08196-5	Quartz	I	15.1	8.5	304	−69.2	
S09132-10	Quartz	I	14.2	8.3	327	−71.5	
S05232-13-a	Quartz	II	14.6	6.7	273	−71.1	
S07217-II-2	Quartz	II	13.1	5.3	274	−73.8	
S09132-3-a	Quartz	II	14.6	6.9	276	−72.0	
S08196-16	Quartz	III	14.3	5.0	239	−79.5	Wang, 2016
S09132-19	Quartz	III	14.9	5.8	244	−71.2	
S05232-13-b	Calcite	IV	11.4	3.6	273	−82.1	
S09132-3-b	Calcite	IV	12.2	4.9	287	−80.9	
S09132-18	Calcite	IV	12.0	1.9	226	−80.8	
S09132-20	Calcite	IV	12.0	1.0	209	−74.4	

Sanshandao Au Deposit (Wang et al. 2016). Pyrite and sphalerite from Mineralization Stage III have $\delta^{34}S$ values of 11.5‰ and 10.9‰ respectively. Pyrite from Mineralization Stage IV has ^{34}S=10.9‰. The results show that different mineralization stages have similar $\delta^{34}S$ values, which are much higher than those of Jiaodong Group rocks (7.2‰–7.6‰, Yang, 1998). But the value is similar to that of rock delta$\delta^{34}S$ in jingshan group (9.3‰–9.8‰, Deng, 2015). The Guojialing and the Linglong Granites have lower $\delta^{34}S$ values (4‰–8‰) within the region. Mafic dykes have $\delta^{34}S$=4‰–6‰.

The Pb istopic tests of gold deposits in the Jiaodong area indicate that rocks and Au ores of the Jiaodong Group have similar Pb isotopic values, all of which evenly fell within the orogenic-belt and lowe crustal Pb fields. This suggests that these rocks and ores are closely correlated in genesis (Lin, 1999).

5.4 Sources of ore-forming elements

In the Mesozoic time, the Yangtze Plate collided with the North China Plate, whereas the Pacific Plate subducted beneath and extruded the Eurasian Plate and deeply incised the Yishu fault of the upper mantle. These phenomena led to large-sized sinistral strike-slipping and subsequent complex activity associated with widespread tectono-magmatic hydrothermal events. The bedded crust-derived re-melting Linglong granites formed in the Late Jurassic time, leading to Au activation, dispersion, and migration in primary ore sources (pre-Cambrian meta-basement rocks). The participated high-temperature hydrothermal solution dissolved ore-forming elements (such as Au), forming an initial Au-bearing hydrothermal solution. The Linglong-type granites are considered the derived ore source rock series of Au mineralization (Li et al., 2007). With lithosphere thinning and mantle material upwelling, the Guojialing-type granodiorites, which are mainly of crustal and mixed crust–mantle sources, formed in the early Cretaceous period; the post-magmatic hydrothermal solution provided a main heat source and ore -forming fluids for Au mineralization and played a key role in mineralization. Au-rich multi-sourced ore-forming fluids entered into structural fissure systems and altered and replaced wall rocks, thereby increasing the concentration of ore-forming elements in ore-bearing hydrothermal solution. With the uplift of intrusions and decrease in temperature, injection of meteoric water quickened Au precipitation, forming a series of gold deposits (Fig. 8) (Yang et al., 2012). The ore-forming fluids of Au deposits in the Jiaodong area are of mixed crust–mantle origin and dominated by crust-derived fluids; the ore-forming elements were generally sourced from pre -Cambrian metamorphic basement rocks and mixed with minor shallow crustal and mantle components (Tan et al., 2012; Yang et al., 2014).

6 Conclusions

(1) Fluid inclusions of pyrite from the Sanshandao Au deposit have $^{3}He/^{4}He$=0.043–0.21Ra with an average of 0.096 Ra and $^{40}Ar/^{36}Ar$=488–664 with an average of

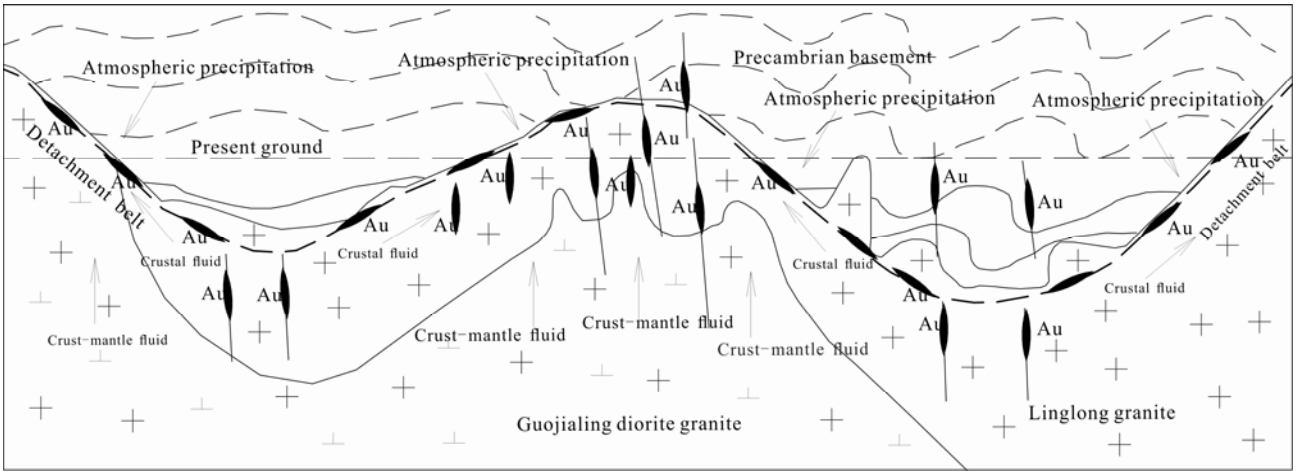


Fig. 8. The diagram of ore-forming fluids from gold deposits in the Jiaodong area.

570.8. These values basically reflect the primary He and Ar isotopic compositions of ore-forming fluids when fluid inclusions were captured.

(2) He and Ar isotopic compositions of ore-forming fluids of the Sanshandao Au deposit indicate that the ore-forming fluids display mixed crust–mantle signatures, dominated by crustal fluids, with minor mantle-derived fluids.

(3) Combined with deposit geology, wall rock alteration, fluid inclusions, and isotopic evidence, the ore-forming fluids of the Sanshandaod Au deposit display mixed crust–mantle signatures, with minor meteoric water during uprising of the ore-forming fluids. The ore-forming elements were generally sourced from pre-Cambrian meta-basement rocks formed by Mesozoic reactivation and mixed with minor shallow crust and mantle components.

Acknowledgements

This study was funded by Demonstration of Three-Dimensional Prospecting Evaluation for Deep Mineral Resources (Grant No. 2017YFC0601506), Comprehensive study of the whole gold exploration area in Laizhou to Zhaoyuan (2014-7) and Investigation of Mesozoic granites in Jiaodong area and its relationship with gold deposits (2018-19). Field work has been assisted and supported by relevant staff of Sanshandao Gold Deposit. Thanks Liwu Wang and Chunhui Cao from Lanzhou Center for Oil and Gas Resources, Institute of Geology and Geophysics, CAS for sample testing.

Manuscript received Jan. 29, 2019
accepted Mar. 14, 2019
associate EIC FEI Hongcai
edited by LIU Lian

References

Burnard, P.G., Hu, R., Turner, G., and Mantle. 1999. Crustal and atmospheric noble gases in Ailaoshan Gold deposits,Yunnan Province, China. Geochimica et Cosmochimica Acta, 63 (1999): 1595–1604.

Cao, C.H., Z, M.J., T, Q.Y., Y, Y., L, Z.G., Z, T.W., C, C., Y, H., and L, L.W. 2018. Noble gas isotopic variations and geological implication of Longmaxi shale gas in Sichuan Basin, China. Marine and Petroleum Geology, 89(2018): 38–46.

Deng, J., Yang, L.Q., Fang, Y., Ding, S.J., Wang, J.P., and Meng, Q.F. 2000. Crust-mantle interaction and ore-forming effect of gold ore deposits concentrated area in Jiaodong, Shandong, China. Scientia Geologica Sinca, 35(1): 60–70 (in Chinese).

Deng, J., Liu, X.F., Wang, Q.F., and Pan, R.G. 2015. Origin of the Jiaodong-type Xinli gold deposit, Jiaodong Peninsula, China: Constraints from fluid inclusion and C–D–O–S–Sr isotope compositions. Ore Geology Reviews, 65(2015): 674–686.

Duan, C., Liu, F., Han, D., and Li Y.H. 2016. Noble gas isotope analytical techniques and its application in economic geology researches. Acta Geologica Sinica, 90(8): 1908–1921 (in Chinese).

Fan, H.R., Hu, F.F., Yang, J.H, Shen, K., and Zhai, M.G. 2005. Fluid evolution and large-scale gold metallogeny Mesozoic tectonic transition in eastern Shandong Province. Acta Petrologica Sinica, 21(5): 1317–1328 (in Chinese).

Hu, R.Z., Bi, X.W., Turner, G., and Burnard, P. 1999. Isotope geochemistry of He and Ar in ore-forming fluid of Ailaoshan gold mineralization belt. Science in China (Series D), 29(4): 321–330 (in Chinese).

Hu, F.F., Fan, H.R., Zhai, M.G., and Jin, C.W. 2006. Fluid evolution in the Rushan lode gold deposit of Jiaodong Peninsula, eastern China. Journal of Geochemical Exploration, 89 (2006): 161–164.

Hacker, B.R., Wallis, S.R., Mcwilliams, M.O., and Gans, P.B. 2009. $^{40}Ar/^{39}Ar$ Constraints on the tectonic history and architecture of the ultrahigh-pressure Sulu orogeny. J. metamorphic Geol., 27(2009): 827–844.

Jiao, X.Y., Fan, X.L., Yu, P.H., Jiang, H.H., Xiong, W.B., Cheng, Z.Y., and Ma, J.L. 2016. He-Ar isotopic system of fluid inclusions in pyrite from the Changba lead-zinc deposit in Gansu Province. Gold Science and Technology, 24(4): 47–53 (in Chinese).

Kendrick, M.A., Burgess, R., Pattrick, R.A.D., and Turner, G. 2001. Fluid inclusion noble gas and halogen evidence on the original of Cu—Porphyry mineralizing fluids. Geochimica et Cosmochimca Acta, 65(16): 2651–2668.

Li, H.Q., Liu, J.Q., and Wei, L. 1993. Geochronology and geological application of fluid inclusions in hydrothermal deposits. Beijing: Geological publishing house, 1–125.

Li, H.Z., Yang, H.Q., Wang, D.H., Ren, S.L., and Li, Y.B. 1995. A new method based on neural network molding for finding gold desposits in Jiaodong greenstone belt. Geology of Shandong, 11(1): 63–67 (in Chinese).

Li, S.X., Liu, C.C., An, Y.H., Wang, W.C., Huang, T.L., and Yang, C.H. 2007. Geology of gold deposits in Jiaodong. Beijing: Geological publishing house, 1–423.

Li, X.F., Mao, J.W., Wang, Y.T., and Wang, D.H. 2003. Evidence of noble gas isotopes and halogen for the Origin of ore-forming fluids. Geological Review, 49(5): 513–521 (in Chinese).

Li, X.F., Mao, J.W., Wang, D.H., and Luo, F.X. 2004. Helium and Argon isotope systematics in fluid inclusion of the gold deposits along the Daduhe River, Sichuan Province, Southwestern China. Acta Geologica Sinica, 78(2): 203–210 (in Chinese).

Li, Y.F, Mao, J.W., Hu, H.B., Bai, F.J., Li, H.M., Li, M.W., Guo, B.J., and Ye, H.C. 2005. The Fluid Inclusions and Their He-Ar-S-H-O Istopic Compositions and Tracing to the Source of Ore-Forming Fluids for the Gongyu Gold Deposit, Western Henan. Acta Petrologica Sinica, 21(5): 1347–1358 (in Chinese).

Lin, W.W., Zhao, Y.M., Zhao, G.H., and Zhao, W.G. 1999. Discussion on geological characteristics of lead isotope and metallogenic age in Jiaodong gold deposit.Journal of Changchun University of Science and Technology, 29(2): 116–121 (in Chinese).

Mamyrin, B.A., and Tolstikhin, I.N. 1984. Helium Isotopes in Nature. Amsterdan and New York: Elsevier Science Publishers, 38–165.

Mao, J.W., Li, Y.H., Li, H.Y., Wang, D.H., and Song, H.B. 1997. Helium isotopic evidence on metalgenisis of mantle fluids in the Wangu gold deposit Hunan Province. Geological Review, 43(6): 646–649 (in Chinese).

Mao, J.w., and Wei, J.X. 2000. Helium and argon isotopic components of fluid inclusions and tracing to the source of metallogenic fluids in the Dashuigou tellurium deposit of Sichuan Province. Acta Geoscientia Sinica, 21(1): 58–61 (in Chinese).

Mao, J.W., Li, X.F., Zhang, R.H., Wang, Y.T., Hao, Y., Zhang, Z.H., and Ling, H.F. 2005. Mantle-derived fluid-related ore-forming system. Beijing: China Land Publishing House, 95–120.

Mao, J.W., Wang, Y.T., Li, H.M., Franco, P., Zhang, C.Q., and Wang, R.T. 2008. The relationship of mantle-derived fluids to gold metallogenesis in the Jiaodong Peninsula: Evidence from D–O–C–S isotope systematics. Ore Geology Reviews, 33 (2008): 361–381.

Shen, B.F, and Luo, H. 1994. The metallogenetic characteristics of gold deposits of the archean greenstone belts in North China platform. Jour Geol and Min Res North China, 1994(1): 87–96 (in Chinese).

Song, M.C. 2015. The main achievements and key theory and methods of deep-seated prospecting in the Jiaodong gold

concentra–tion area, Shandong Province. Geological Bulletin of China, 34(9): 1758–1771 (in Chinese).
Song, M.C., Zhang, J.J., Zhang, P.J., Yang, L.Q., Liu, D.H., Ding, Z.J., and Song, Y.X. 2015. Discovery and Tectonic-Magmatic Background of Superlarge Gold Deposit in Offshore of Northern Sanshandao, Shandong Peninsula, China. Acta Geologica Sinica, 89(2): 365–383 (in Chinese).
Stuart, F.M., Burnard, P.G., and Taylor, R.P. 1995. Resolving mantle and crustal contributions to ancient hydrothermal fluids: He-Ar isotopes in fluid inclusions from Dae Hwa W-Mo mineralisation, South Korea. Geochimica et Cosmochimica Acta, 59(22): 4663–4673.
Tan, J., Wei, J.H., Andreas, A.T., and Thomas, P.K. 2012. Source of metals in the Guocheng gold deposit, Jiaodong Peninsula, North China Craton: Link to early Cretaceous mafic magmatism originating from Paleoproterozoic metasomatized lithospheric mantle. Ore Geology Reviews, 48 (2012): 70–87.
Tian, J.P., Tian, J.X., Guo, R.P., Wei, C.S., Wang, L.G., Yu, X.W., Li, X.Z., Huang, Y.B., Zhang, C.C., Liu H.D., and Zhu, P.G. 2016. Jiaodong-type gold deposit related to crust source remelting layered granite and crust-mantle mixed granodiorite. Acta Geologica Sinica, 90(5): 987–996 (in Chinese).
Yang, Q.l., Zhao, Z.F., and Zheng, Y.F. 2012. Slab–mantle interaction in continental subduction channel: Geochemical evidence from Mesozoic gabbroic intrusives in southeastern North China. Lithos, 155(2012): 442–460.
Yao, F.L., Liu, L.D., Kong, Q.C., and Gong, R.T. 1990. Gold lodes in the northwestern part of the Jiaodong. Changchun: Jilin Science and Technology Press, 1–189.
Ye, X.X., Wu, M.B., and Sun, M.L. 2001. Determination of the Noble Gas Isotopic Composition in Rocks and Minerals by Mass Spectrometry. Rock and Mineral Analysis, 20(3): 174–178 (in Chinese).
Yang, L.Q., Deng, J., Wang, Z.L., Zhang, L., Guo, L.N., Song, M.C., and Zheng, X.L. 2014. Mesozoic gold metallogenic system of the Jiaodong gold province, eastern China. Acta Petrologica Sinica, 30(9): 2447-2467 (in Chinese).
Yang, L.Q., Deng, J., Goldfarb Richard, J., Zhang, J., Gao, B.F., and Wang, Z.L. 2014. $^{40}Ar/^{39}Ar$ geochronological constraints on the formation of the Dayingezhuang gold deposit: New implications for timing and duration of hydrothermal activity in the Jiaodong gold province, China. Gondwana Research, 25 (2014): 146–1483.
Yang, J.H., Zhou, X.H., and Chen, L.H. 2000. Dating of gold mineralization for super-large altered tectonite-type gold deposits in Northwestern Jiaodong Peninsula and its implications for gold metallogeny. Acta Petrologica Sinica, 16 (3): 454-458 (in Chinese).
Wang, Z.L., Yang, L.Q., Guo, L.N, Marsh, E., Wang, J.P., Yue, L., and Zhang, C. 2014. Fluid immiscibility and gold deposition in the Xincheng deposit, Jiaodong Peninsula, China: A fluid inclusion study. Ore Geology Reviews, 3 (2015): 701-717.
Zhai, M.M., Yang, J.H., and Liu, W.J. 2001. Large-scale gold concentration area and large-scale metallogenesis in Jiaodong. Science in China (Series D), 31(7): 545–552 (in Chinese).
Zhang, L.G., Chen, Z.S., Liu, J.X., Yu, G.X., Wang, B.C., Xu, J.F., and Zheng, W.S. 1994. Water-rock exchange in the Jiaojia type gold deposit: a study of hydrogen and oxygen isotopic composition of ore-forming fluids. Mineral Deposits, 13(3): 193–200 (in Chinese).
Zhang, L.C., Shen, Y.C., Li, H.M., Zeng, Q.D., Li, G.M., and Liu, T.B. 2002. Helium and argon isotopic compositions of fluid inclusions and tracing to the source of ore-forming fluids for Jiaodong gold deposits. Acta Petrologica Sinica, 18(4): 559–565 (in Chinese).
Zhang, L., Li, G.G., Zheng, X.L., An, P., and Chen, B.Y. 2016. $^{40}Ar/^{39}Ar$ and fission-track dating constraints on the tectonothermal history of the world-class Sanshandao gold deposit, Jiaodong Peninsula, eastern China. Acta Petrologica Sinica, 32(8): 2465–2476 (in Chinese).
Zhu, L., Zhang, G., Guo, B. and Li, B. 2009. He-Ar isotopic system of fluid inclusions in pyrite from the molybdenum deposits in south margin of North China Block and its trace to metallogenetic and geodynamic background. Chinese Science Bulletin, 54(12): 1725–1735 (in Chinese).

About the first author



HAN Zhenyu, male, born in 1986, in Dezhou City, Shandong Province; Ph.D.candidate in Shandong University of Science and Technology. His research focuses on Geological and Mineral Exploration. Email: 469513762@qq.com; phone: 15853557763.

About the corresponding author



LI Shoujun, male, born in 1962, in Weifang City, Shandong Province, professor in Shandong University of Science and Technology. He is engaged in the study of geology. Email: lishoujun@126.com; phone:13789879228